α-alumina as catalyst support in Co Fischer-Tropsch synthesis and the effect of added water; encompassing transient effects

Erling Rytter, [a,b] Øyvind Borg, [ϕ,a] Bjørn Christian Enger [b] and Anders Holmen*[,a]

[a] Department of Chemical Engineering, Norwegian University of Science and Technology (NTNU), N-7491 Trondheim, Norway

[b] SINTEF Industry, N-7465 Trondheim, Norway

Abstract

Three catalyst supports containing from 84 to 100% α-alumina prepared by heat treatment of γ-alumina have been impregnated with cobalt and rhenium. The catalysts were tested for Fischer-Tropsch synthesis (FTS) under dry and enhanced water vapor pressure conditions. Both activity and selectivity to higher hydrocarbons respond positive to water added or generated *in situ* by the reaction. A linear trend between formation of methane and C_{5+} products were found, but displaced to higher C_{5+} values compared to catalysts on γ-alumina. Calculation of chain propagation probabilities (α_n) for α-alumina supported catalysts discloses that the first step, characterized by α_1, increases the most under higher water partial pressure. Moreover, α_1 is significantly higher for α- compared to all γ-alumina supports irrespective of pore sizes of the latter. These results are ascribed to suppression of hydrogen coverage on the cobalt surface, linked to more regular cobalt crystallites, accompanied by enhanced water assisted generation of CH_x polymerization monomers. Surprisingly, the following α_2 probability is comparably low for α-alumina supports, although it increases significantly with water concentration. Linear correlations are found between each pair of parameters α_1, α_2, α_4 and S_{C5+}; giving support to a mechanistic model where all products are interlinked, including methane. Transients observed when water was added or removed from the system are ascribed to pore diffusion. Selectivities in these periods follow closely the general selectivity trends found for different process conditions.

[ϕ] Present address: Equinor Research Center, Trondheim, Norway

Introduction

Supported cobalt catalysts are widely studied and applied for conversion of synthesis gas in low-temperature (< 250 °C) Fischer-Tropsch (FT) synthesis (FTS). These catalysts are characterized by high FT activity, high selectivity to long chain paraffins and low-water-gas shift activity. It is common practice to add a noble metal promoter, typically platinum or rhenium, to optimize the performance of the catalyst. The catalyst activity largely depends on the degree of reduction of the cobalt metal precursor and the size of the cobalt crystallites, which control the number of catalytically active sites that are available (dispersion). It has also been shown that the TOF (turn over frequency, *i.e.* CO hydrogenations per active site and time) is reasonably constant for Co particles larger than 5-6 nm.[1,2] However, the TOF is sensitive to the support (catalyst carrier), *e.g.* α-alumina and certain aluminates (spinels) show higher activity than γ-alumina for catalysts that have the same Co crystallite size.[3] Some efforts have been made to describe the actual shape and distribution of the cobalt particles or their oxide precursors, but so far it has been challenging to correlate this information with catalytic properties.[4,5] It has also been claimed that cobalt being in the *hcp* or *fcc* phase is important, with *hcp* being the more active.[6] A structural model was proposed recently by Tsakoumis *et al.* in an investigation on the *hcp* and *fcc* phases of cobalt in FTS.[7] It was shown that crystals with less defects, possibly due to absence of stacking faults, are beneficial for high activity and selectivity. The conclusions were based on examination of catalysts on both γ-alumina and α-alumina supports by XRD and XANES.

The most frequently used activity and reduction promoters are rhenium, platinum or ruthenium, although numerous others have been investigated. Rhenium was first reported added to a Co/titania catalyst,[8] and shortly after to Co/γ-alumina.[9] Mauldin and Varnado concluded that for the former system rhenium functions to increase cobalt oxide dispersion during catalyst preparation and to promote reduction of cobalt oxide to the active metal phase.[10] A similar conclusion was reached for the alumina supported system by Hilmen *et al.*[11] Diehl and Khodakov have reviewed promotion of cobalt FT-catalysts with noble metals.[12]

The type and structure of the support influence the dispersion and consequently the properties of the FT-catalyst systems. The most frequently used supports described in the literature are alumina, silica and titania.[13] These materials behave differently when cobalt is deposited and, equally important, there are huge differences in properties within each class of support. These differences result in variations in activity, but to a larger extent in the polymerization probability, *e.g.* as detected by the C_{5+} selectivity.[14,15,16,17] Supports like titania, α-alumina and certain aluminates yield significantly higher selectivities than silica and γ-alumina. Further, for all catalyst systems and process conditions, water added to the feed and water produced during FT synthesis give higher selectivity to higher hydrocarbons. Therefore, the C_{5+} selectivity increases with conversion due to the positive effect of indigenously produced water. Above 80 % conversion the selectivity drops as the water-gas-shift (WGS) reaction significantly increases the hydrogen concentration, presumably due to oxidation of cobalt.[18]

In a recent paper it was suggested that water plays a key role in activation of CO by providing hydrogen to the oxygen atom.[19] Adsorbed water interacts with CO and presumably lowers the energy barrier for CO activation, thereby enhancing the surface coverage of polymerization monomers CH_x. Added water to the syngas feed may increase or decrease the catalyst activity.[20] More inert supports and large pore sizes have a positive response. Most notable exceptions are medium to narrow pore size γ-alumina and silica that has a negative response to water.[21] Further, there is a limit to the positive effect of water on activity as too high amounts result in decreased activity; most likely due to oversaturation of the cobalt surface with water molecules or hydroxyl. In a similar approach, it has

been proposed that water acts as a "H-shuttling mediator" that facilitates hydrogenation of CO through a $H_3O^{\delta+}$ type intermediate.[22,23]
It is challenging to describe the detailed pore structure of the support and the distribution of cobalt in the pores. The average properties of alumina, on the other hand, like pore size distribution, surface area, average pore diameter and pore volume, can easily be measured. It is likely that the pore geometry influences the catalytic properties, in addition to factors like the purity of the support and the phase.[24,25] It has been reported that for comparable γ-aluminas with surface areas in the range 170-200 m^2/g, the C_{5+}-selectivity increases with pore volume and pore diameter.[25,26] There appears to be a limit to the size effect, and the selectivity levels out at ca. 10 nm,[2] and even a decline is found for large crystals.[27] It is intriguing, however, that even when controlling the cobalt crystal size, different alumina phases show varying selectivities.

Iglesia and co-workers investigated a Co/SiO_2 catalyst for the responses of water and found that both CO formation rate and C_{5+} selectivity increase by adding water to the feed.[28] By adding water during FTS for 13 different γ-alumina supports, with large variations in pore sizes and pore size distributions, some important correlations were found.[29] It was shown that due to a positive correlation between pore size and cobalt crystallite size, as long as the pore size distribution is sufficiently narrow, there is a concurrent increase in C_{5+} with pore diameter. This increase in selectivity was found due to higher chain propagation probabilities α_{3+}. High α values were ascribed to large cobalt crystallites that promote CO activation with consequently higher surface coverage of CH_x monomers. Increase in cobalt crystallite size and degree of reduction with increasing pore diameter was also detected when using a silica support.[30] In addition, a close correlation was found between positive responses to water for C_{5+} selectivity and CO conversion,[29] pointing at the same mechanistic origin. Added water imposes a significant enhancement of α_1, *i.e*. the probability for chain initiation *vs*. termination to methane. This was attributed to higher relative cobalt surface coverage of water or hydroxyl and CH_x monomers relative to hydrogen. Visconti and co-workers testes cobalt catalysts on a γ-alumina support during extended tests up to 1000 h time-on-stream and with water added to the feed.[31] Their results comply with the observations and conclusions above, but they were also able to conclude on a reduction in alcohol selectivity. Some selectivity responses were reversible and some irreversible. Essentially, the results were explained by suppression of hydrogen activity.

Alumina is the most intensively investigated support for Co FT-catalysis. On γ-alumina it is commonly assumed that a fraction of the cobalt forms an irreducible cobalt aluminate spinel covering most of the surface.[32] Intrusion of Co^{II} into the alumna lattice has been observed to occur during reduction.[33] Although γ-Al_2O_3 is the standard alumina-based catalyst carrier, several transition phases occur during calcination before the thermodynamically stable α-alumina phase is reached. The crystal morphology of alumina is rather complex, and a large number of polymorphs exist and are formed upon dehydration. Transition between the different phases is not particularly transparent. Boehmite has the formula AlO·OH while Bayerite is a form of Gibbsite; $Al(OH)_3$. Starting from Diaspore (AlO·OH) the χ and κ phases are obtained by heat treatment. Most relevant for the present study are the γ- and α-phases obtained by dehydration of Boehmite. Transition through the phases δ-Al_2O_3 and θ-Al_2O_3 is achieved by calcination until α-Al_2O_3 is obtained at temperatures exceeding 1100 °C. γ-Al_2O_3 is regarded as a defect spinel in that it is based on the spinel structure, but with a deficit of cations. α-Al_2O_3 contains a closed packed array of oxygen atoms with aluminum distributed regularly among the octahedral interstices. It has been shown that successive high temperature calcination accompanied by changes in pore geometry and partial transformation of γ- Al_2O_3 to α- Al_2O_3 gives catalysts with significant increase in selectivity.[34,35] Such treatment drastically reduces the alumina surface area, from typically 150-200 m^2/g to 5-15 m^2/g, and the dispersion and distribution of cobalt thereby becomes restricted by the low available surface area. The shape of the support crystals

changes drastically during calcination from flakes or needles to large, almost cubic forms, as seen in 3D and *in situ* TEM.[36,37]

Previously, we suggested that the effects of support material and pore dimension have the same origin.[38] According to this model, both should directly or indirectly determine the concentration and composition of a pool of CH_x species on the cobalt surface. A common denominator between support and pore size is that improved C_{5+} selectivity is found for supports composed of larger crystals, *i.e.* low surface area materials. Alumina and aluminate data complied with titania- and silica-based catalysts in this respect. Combined with TEM data that indicate cobalt crystallites to bend over alumina crystallites,[39] it was proposed that less strained Co crystals are formed on low surface area supports like α-alumina and in larger pores; an extension of the cobalt crystallite size effect. Strain in Ni crystals on carbon nanofibers as analyzed by XRD line broadening has been shown to impact TOF for hydrogenolysis of ethane as well.[40] For narrow pore γ-alumina, cobalt crystals extend over several crystallites of the support whereas α-alumina has large enough crystals to easily accommodate unstrained cobalt-crystallites. It was argued that strain, used in a broad sense, influences the CH_x pool. The strain model complies well with observations of pool composition with variation in cobalt crystallite size.[41] Certainly, small crystallites are more prone to strain and edge effects.

The present work concentrates on α-alumina as support. Effect of water is studied by adding water vapor during the FT-reaction. An attempt is made to unravel the relationship between alumina support type and cobalt size with water response and selectivity.

Experimental

Catalyst preparation. Laboratory catalysts were prepared as described previously.[25,42] Three different α-Al_2O_3 supports were prepared by calcination of γ-Al_2O_3 (Puralox SCCa 45/190; Sasol GmbH) for 16 h in a static furnace using a heating rate of 5 °C/min to a final holding temperature as detailed in Table 1. The catalyst cobalt oxide precursor was prepared by one-step incipient wetness co-impregnation with an aqueous solution of cobalt nitrate hexahydrate and perrhenic acid. Great care was taken to use chemicals with high purity only. The support and metal solution were mixed under ambient temperature and pressure conditions. Before impregnation, the support (53-90 µm) was calcined under air at 500 °C for typically 10 h in a static furnace. This re-calcination procedure is included to equilibrate the surface hydroxyl concentration of different samples after storage. The catalysts contain a nominal amount of 20 or 12 wt% cobalt and 0.5 wt% Re, as calculated assuming reduced catalyst with complete reduction of cobalt. ICP analysis of calcined samples showed cobalt content in the 16.3-18.9 wt% range and rhenium between 0.36 and 0.42 wt%. After impregnation, the catalyst precursor was dried in a stationary oven at 110-120 °C for 3 h. To ensure homogeneity, the sample was stirred gently every 15 min the first hour and every 30 min the last two. After drying, calcination was performed at 300 °C for 16 h in a static furnace, with a heating rate of 2 °C/min to the holding temperature. Both ramp rate, holding temperature and time, gas composition (humidity) and gas flow rate influence particularly the cobalt crystallite size and thereby optimization and reproducibility of the Fischer-Tropsch performance.[43]

Table 1. Prepared alumina supports and cobalt catalysts.

Sample	Type of material	Calcination temperature (°C)	α-alumina (%) / Co/Re (wt%)	Surface area (m^2/g)	Co particle size [a] (nm)	Dispersion (%) [a]

S_γ [b]	γ-alumina	500	0	191	-	-
$S_{\alpha1}$	α-alumina	1130	84	16.8	-	-
$S_{\alpha2}$	α-alumina	1134	96	n.a.	-	-
$S_{\alpha3}$	α-alumina	1140	100	10.3	-	-
C_γ [b]	Co/Re on S_γ	-	20/0.5	149	12.3	7.82
$C_{\alpha1}$	Co/Re on $S_{\alpha1}$	-	20/0.5	23,5	19.0	3.66
$C_{\alpha2}$	Co/Re on $S_{\alpha2}$	-	20/0.5	15,3	22.5	1.59
$C_{\alpha3}$	Co/Re on $S_{\alpha3}$	-	12/0.5	17.8	20.5	2.78

[a] From hydrogen chemisorption.

[b] Corresponds to S_{10} and C_{10}, respectively, in previous reports.[25,29]

Fixed-Bed Catalyst Testing. The Fischer-Tropsch reactions were conducted in a fixed-bed reactor (stainless steel, 10 mm inner diameter). The apparatus is partly automated with two reactors in parallel. The samples were sieved (53-90 µm) and 1-2 g were diluted with inert silicon carbide particles (20.0 g, 75-150 µm) in order to improve the temperature distribution along the catalytic zone. An aluminum jacket was placed outside the reactor to secure isothermal conditions. The catalyst was reduced *in situ* in hydrogen at ambient pressure while the temperature was increased at 1 °C/min to 350 °C. After 16 h of reduction, the reactor was cooled to 170 °C under hydrogen. The system was then pressurized to 20 bar under equal flow rates of hydrogen and helium, where after hydrogen was exchanged with helium. Synthesis gas of molar ratio $H_2/CO = 2.1$ with 3% N_2 as an internal standard was introduced, and the temperature increased slowly to the reaction temperature of 210 °C. Space velocity was adjusted according to a reactor model to give a predicted carbon monoxide conversion level between 45 and 50 percent after 26 h time on stream (TOS). Water was vaporized, heated to reaction temperature and added to the feed at intervals in two concentration levels, 4.25 bar and 7.06 bar; simulating 46 and 64% conversion at the inlet, respectively.

Liquid products were removed in a cold trap, while heavy hydrocarbons were collected in a heated trap. The effluent gaseous product was analyzed for hydrogen, nitrogen, carbon monoxide, carbon dioxide, water, and C_1 to C_9 hydrocarbons using an HP5890 gas chromatograph equipped with a thermal conductivity detector (TCD) and a flame ionization detector (FID). The C_{5+} selectivity was calculated by subtracting the amount of C_1-C_4 hydrocarbons and carbon dioxide in the product gas mixture from the total mass balance. Activity is reported as the hydrocarbon formation rate ($g_{\text{hydrocarbon}}/(g_{\text{catalyst}}h)$). The precision of the activity is 3% (2σ). To check for particle external mass transfer limitations, experiments with different catalyst loading, but constant diluted bed heights, were performed. The catalyst space velocity was unaltered, thereby operating at varying linear velocities. Selectivities at constant conversion measured after 100 h TOS show minimal variations.

Catalyst Characterization. Nitrogen adsorption/desorption isotherms were measured after outgassing at 300 °C overnight. The surface area was calculated from the Brunauer-Emmett-Teller (BET) equation, and total pore volume and pore size distribution were found by applying the Barrett-

Joyner-Halenda (BJH) method.[44] The nitrogen desorption branch was chosen for pore size analysis. Hydrogen adsorption isotherms were obtained after evacuation at 40 °C for 1h followed by reduction in hydrogen for 6h at 350 °C. Chemisorbed hydrogen was found from the isotherm recorded in the pressure interval 20 to 510 mmHg and extrapolation to zero pressure. Cobalt crystallite size was calculated by assuming spherical particles and no contribution from the rhenium promoter. Oxygen titration of reduced samples was performed by adding a series of oxygen pulses at 400 °C. Degree of reduction (DOR) was calculated assuming that metallic cobalt oxidized to Co_3O_4. Measuring DOR is not trivial, and it has been reported that the present oxygen pulsing technique may underestimate the degree of reduction due to incomplete oxidation.[45] Powder X-ray diffraction patterns were recorded using Cu K_α radiation with wavelength $1.54*10^{-10}$ m. Temperature-programmed reduction (TPR) experiments were performed on calcined samples using a gas consisting of 7% hydrogen in argon and 10 °/min ramping speed.

Details on applied catalyst characterization equipment and procedures can be found in a previous report.[25]

Attrition. A modified ASTM type equipment was used for testing attrition. It consists of two main parts, one air feeding system and one reactor where the attrition takes place. Compressed air passes through a pressure regulator (5 bar) to a moisture chamber where the air is adjusted to approximately 30 % relative moisture. The humid air then enters the reactor through a sieve tray where the holes have a diameter of 0.4 mm. The gas reaches sonic velocity, which causes the “wear and tear” on the particles in the reactor. The reactor has an internal diameter of 35.6 mm and a length of 711 mm, and the pressure is approximately 1.8 bar. Fines produced in the reactor are collected in a Soxhlet filter and weighed every 15 minutes during the first 2 h, and every 30 minutes during the next 3 h.

Results and discussion

Support and catalyst characterization

Dehydration and sintering of γ-alumina during calcination in air give drastic changes in crystal structure and morphology. The data in Table 1 indicate that transformation to the α-phase becomes dominant only above 1100 °C, until full transformation is seen at 1140 °C. There is a concurrent reduction in surface area to a level around or below 10 m^2/g where cobalt no longer occupies pores but decorates the surface of alumina grains. Incipient wetness impregnation always reduces the measured BET surface area for regular high porosity supports, most likely due to partial blocking of pores. α-alumina samples show an opposite effect as the surface area of the cobalt crystals themselves add significantly to the total surface area (Table 1). It is reasonable that $C_{\alpha 2}$ has lower surface area than $C_{\alpha 1}$ due the higher calcination temperature of the support. The subsequent increase in surface area to $C_{\alpha 3}$ is ascribed to higher dispersion of a catalyst with lower cobalt loading; 2.8 vs 1.6%. No doubt, 20 wt% cobalt for these supports forces coalescence during drying and formation of large cobalt crystals.

As illustrated in the XRD diagrams in Figure 1, small crystallites of γ-alumina transform into large α-alumina crystals with distinct XRD peaks. Note that even at 1130 °C there remains traces of transition θ-alumina that has not been completely converted. There evidently is a concurrent increase in pore size along with the heat treatment approaching 150 nm at 1130 °C by using mercury intrusion, implying a pore volume of ca. 0.8 cm^3/g.[34] The Co/Re catalyst on $S_{\alpha 1}$ support exhibits the expected peaks of cobalt oxide.

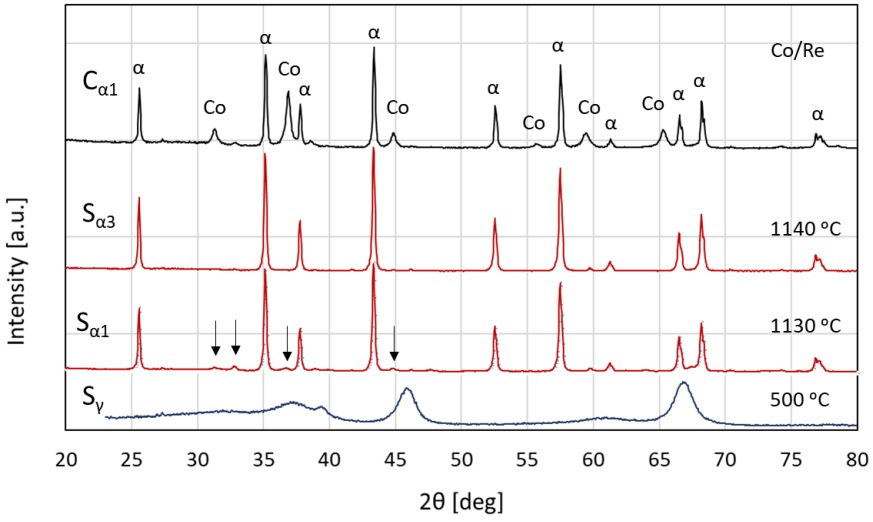

Figure 1. Powder XRD (Cu K_α) of selected supports and one catalyst. Arrows: θ-alumina.

That the transition to α-alumina results in large and inert crystals manifests itself in drastic reduction in surface area and mechanical integrity; see Figure 2. At 1000 °C the surface area is reduced to ⅓, but the α content is moderate with only a slight effect on attrition. Further heating to 1100 °C reduces the surface area significantly to ca. 15 m^2/g with an α content exceeding 80%. Still, there evidently is sufficient transition-alumina left to glue the α-alumina crystals together to some extent. Heating to 1130 °C, and finally to 1140 °C, is needed for full conversion to the α phase with materials that are broken down completely during the air sifting test. The transition can be compared with going from clay or sandstone to sand grains.

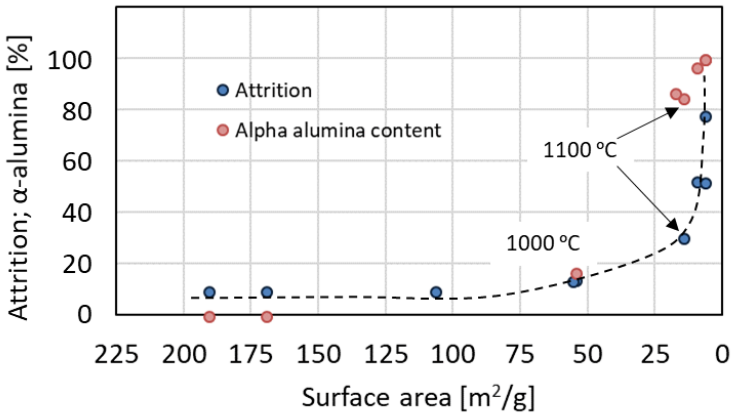

Figure 2. Attrition [%; g/50g] and α-alumina content [%] during calcination at successively higher temperatures as a function of measured surface area. Two series starting with γ-alumina C_7 and C_{10} in previous reports.[25,29]

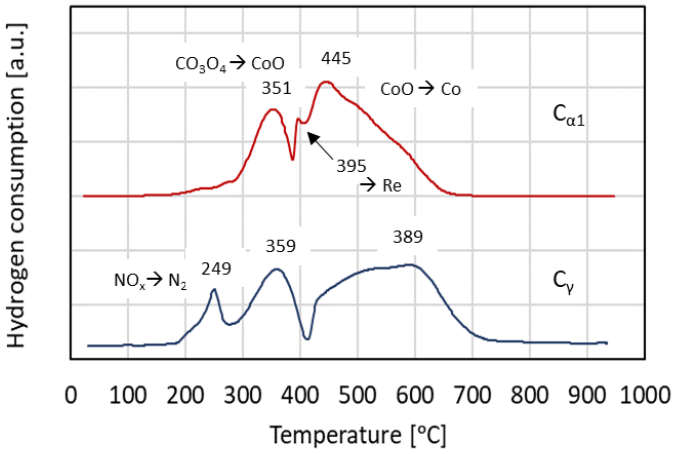

Figure 3. TPR diagrams comparing Co/Re catalysts on γ- and α-alumina.

Comparison of temperature-programmed reduction diagrams of cobalt/rhenium catalysts on γ- and α-alumina is illustrated in Figure 3 and complies well with similar diagrams for catalysts without a promoter.[42] Interpretation of the peaks in terms of cobalt oxide reduction processes is well understood,[25] and have been added to the figure. The main difference in the effect of the two supports lies in reduction of CoO to the metal. As can be expected, the divalent oxide interacts far less strongly with α-alumina. Still, there is a long high temperature tail extending from 500 to 650 °C. This temperature range can be correlated with observed intrusion of Co^{II} into the lattice of γ-alumina during the reduction process.[33] A small sharp peak appears only for catalysts on α-alumina, and we consequently ascribe this feature to reduction of rhenium oxide. It has previously been shown that Re as promoter only shifts the second reduction step of cobalt to lower temperatures.[42] Again it appears that impregnated reagents interact less strongly with the support that contains larger crystals with presumably more relaxed surface energies.

A remark is due the apparent discrepancy between TPR profiles and catalyst reduction temperature. Experience show that reduction at 350 °C is sufficient for activating the catalyst in spite of the apparent extension of the reduction profile to ca. 600 °C. This is expected to be due to the difference between a dynamic experiment with a ramp rate of 10 °C/min compared to static reduction for 16 h. A high reduction temperature would give significant unfavorable sintering of cobalt crystallites and is

therefore avoided. Degree of reduction was found to be 61% for the γ-alumina sample and exceeding 90% for the α-alumina samples, confirming a significant difference in interaction between cobalt and the supports.

Effect of water on catalyst activity

One focus of the present study is on the influence of water on FT performance by adding water during the run. The procedure and effect for the $C_{\alpha 1}$ catalyst is shown in Figure 4. The run is divided into five periods A-E:

A. Synthesis gas with flow rate 250 ml/min.
B. Synthesis gas with reduced space velocity to give an initial CO conversion of ca. 50% at 30 h time-on-stream (TOS).
C. Keeping the synthesis gas flow-rate from period B and adding water vapor to give 21% water vapor pressure at the reactor inlet.
D. Increasing the water vapor pressure to 35%.
E. Returning to the conditions of period B.

This procedure is compatible with previous reports on the effect of water for γ-alumina, silica, titania and carbon nanofiber.[13,21,46,47] The response to water for catalyst $C_{\alpha 1}$ is typical for a low surface area support like titania, and all the three prepared α-alumina catalysts behave very closely to each other. The CO conversion in period C increases initially just after water addition before it levels out at a higher level than in period B. Increased activity follows from the consorted vinylene mechanism encompassing water assisted activation of CO.[19] On the other hand, adding more water gives a slight reduction in conversion; possibly due to oversaturation of the cobalt surface giving reduction in the concentration of polymerization monomers. By adding water, however, the partial pressure of syngas is reduced meaning that the effect on intrinsic activity is larger than shown in the figure.

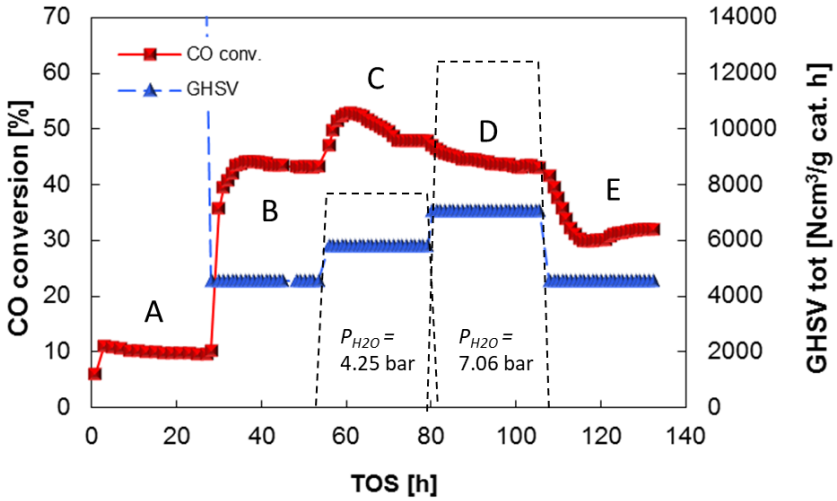

Figure 4. Effect of water addition on CO conversion during FT-synthesis for Co/Re/α-alumina catalyst $C_{\alpha 1}$.

Parallel to the responses to water on activity, catalyst deactivation evidently is occurring. The conversion is reduced from 43% at the end of reference period B to 31% at the beginning of period E;

during just 55 h TOS. The CO conversion in the beginning of period C is 51%, and taking added water into account, this corresponds to the water level that occurs in the outlet of a fixed-bed reactor for a conversion of 74% in dry run; or P_{H20}/P_{H2}=1.3. Similarly, 45 % CO conversion in the start of period D corresponds to 81% conversion for a dry run; P_{H20}/P_{H2}=1.8. These water levels are far higher than normally experienced for fixed-bed FT-synthesis, but the P_{H20}/P_{H2} ratio still is within the operating range for microchannel and slurry bubble column reactors.[20] Therefore, the strongly enhanced deactivation is somewhat surprising. Oxidation of the smallest and most reactive cobalt crystallites is a possibility, consistent with previous TEM studies under similar conditions for γ-alumina supports.[15,48] Further, it is known that sintering is a major cause of deactivation during the initial phase of FT-synthesis,[49,50,51] and sintering most likely is enhanced by water. Formation of aluminates between cobalt and the support is probably also enhanced by water vapor.[52] Although the deactivation is reduced compared to γ-alumina supported catalysts; see Figure 5, it is intriguing that the larger, more regular cobalt crystals deposited on the α phase are prone to such significant oxidation. Nevertheless, in a recent study by Kliewer *et al.* on a Co/Re on titania catalyst,[53] a support that in many respects resembles α-alumina regarding cobalt morphology, they found strong evidence for water induced deactivation due to oxidation of small cobalt particles, cobalt agglomeration and formation of mixed metal oxides. This is in line with the present observations. Note that long-term deactivation due to carbonaceous deposits is likely to occur, but this is probably more relevant at extended run lengths typically in the order of weeks or months.[54]

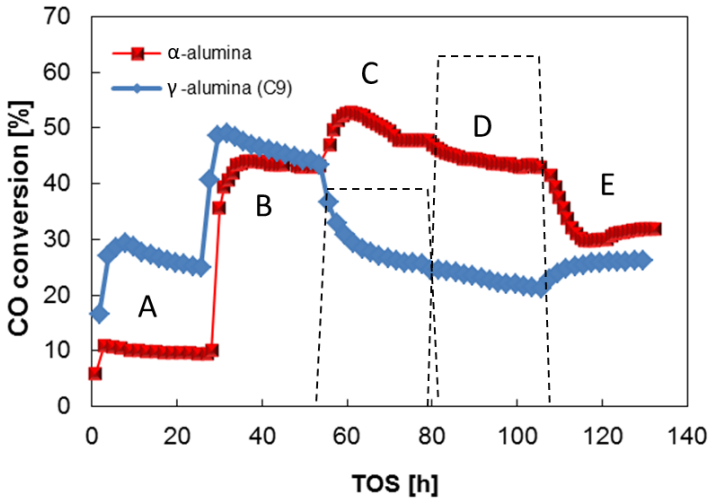

Figure 5. Comparison of the effect of water between catalyst $C_{\alpha 1}$ and catalyst C9 from reference 25.

The difference in behavior upon adding water between γ- and α-alumina supported cobalt catalysts is very visible in Figure 5. Catalyst C9 is characterized by a support with a broad bimodal pore size distribution, and medium average pore (10.4 nm) and cobalt crystallite sizes (9.1 nm).[28] Supports like S_γ, which contains larger pores than C9, show close to neutral effects of water on activity; still far from the enhancement seen for cobalt catalyst on large pore size inert supports.

Effect of water on carbon selectivity

Without exception, there is a positive response of water on C_{5+} selectivity (S_{C5+}), more significant for wide pore size supports.[28] A moderate positive correlation was found between effect of added water on S_{C5+} and average pore size, although there is a better correlation (R^2=0.86) between S_{C5+} and pore

size before extra water is added. The most favorable response to water for catalysts on alumina is by far observed for α-alumina; see Figure 6. Enhancement of longer chains naturally comes at the expense of both the methane and C_2-C_4 fractions due to mass balance of carbon, but methane is most strongly affected. This has been rationalized in terms of a common CH_x pool that provides both monomers for chain growth and species for methanation,[55,56] in addition to a mechanism for CO activation based on water.[19] Added water enhances CO activation with subsequent generation of CH_x that results in higher chain growth probabilities. Simultaneously, water suppresses the hydrogen concentration on the cobalt surface and shifts the composition of the CH_x pool away from methane.

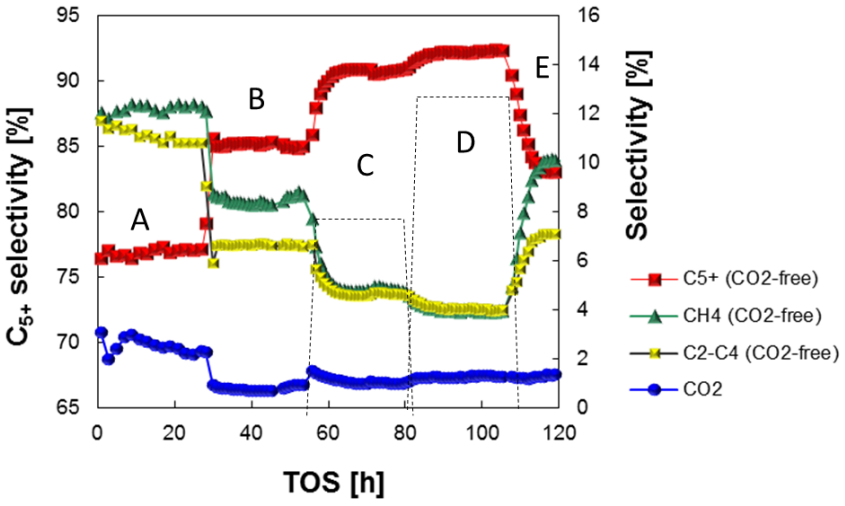

Figure 6. Effect of water addition on carbon selectivities during FT-synthesis for Co/α-alumina catalyst $C_{\alpha 1}$.

Two further observations are significant. First, water in the feed generates more CO_2. This follows from the water-gas-shift (WGS) reaction, although the present conditions are far from equilibrium of this reaction. Note that the CO_2 level is maintained in period E, *i.e.* returning to the initial feed conditions of period B. This observation gives credit to formation of stable cobalt oxides or cobalt aluminates through deactivation, and that this change in surface properties of the catalyst is as relevant as WGS for CO_2 production. Second, methane selectivity is higher in period E than expected, as also found previously for Co/Re/γ-alumina catalysts.[29] More favorable conditions for methanation complies with the opposite found when water was added, discussed above, as lower CO conversion due to deactivation relative to period B provides a syngas leaner in water.

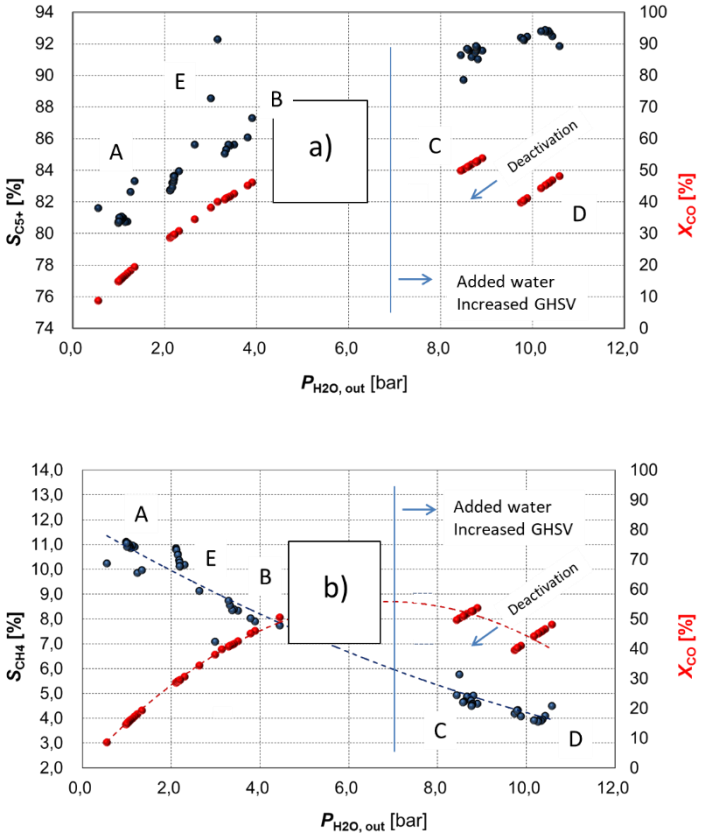

Figure 7. Selectivities and conversion as a function of partial pressure of water for catalyst $C_{\alpha 2}$. a) Selectivity to C_{5+}. b) Selectivity to CH_4.

Figure 7 highlights the effect of water. Selectivities and CO conversion are plotted as a function of water partial pressure at each data point during the run. By definition, conversion partially shows up as a smooth curve as conversion and added water defines the total water pressure. There is slight deviation from a linear trend in dry periods A, B and E due to gas compaction with conversion. A step change in water pressure is naturally seen as steam is added to the feed; this is only partially reflected in an increased conversion. Deactivation shows up as a decline in both conversion and water partial pressure. Methane selectivity follows a gradual decline with water pressure as hydrogen coverage on cobalt is suppressed. Consequently, selectivity to C_{5+} follows the opposite trend but with some deviations; particularly, the transition period in the beginning of period E shows an extraordinary high selectivity to long chain lengths.

Transient water conditions

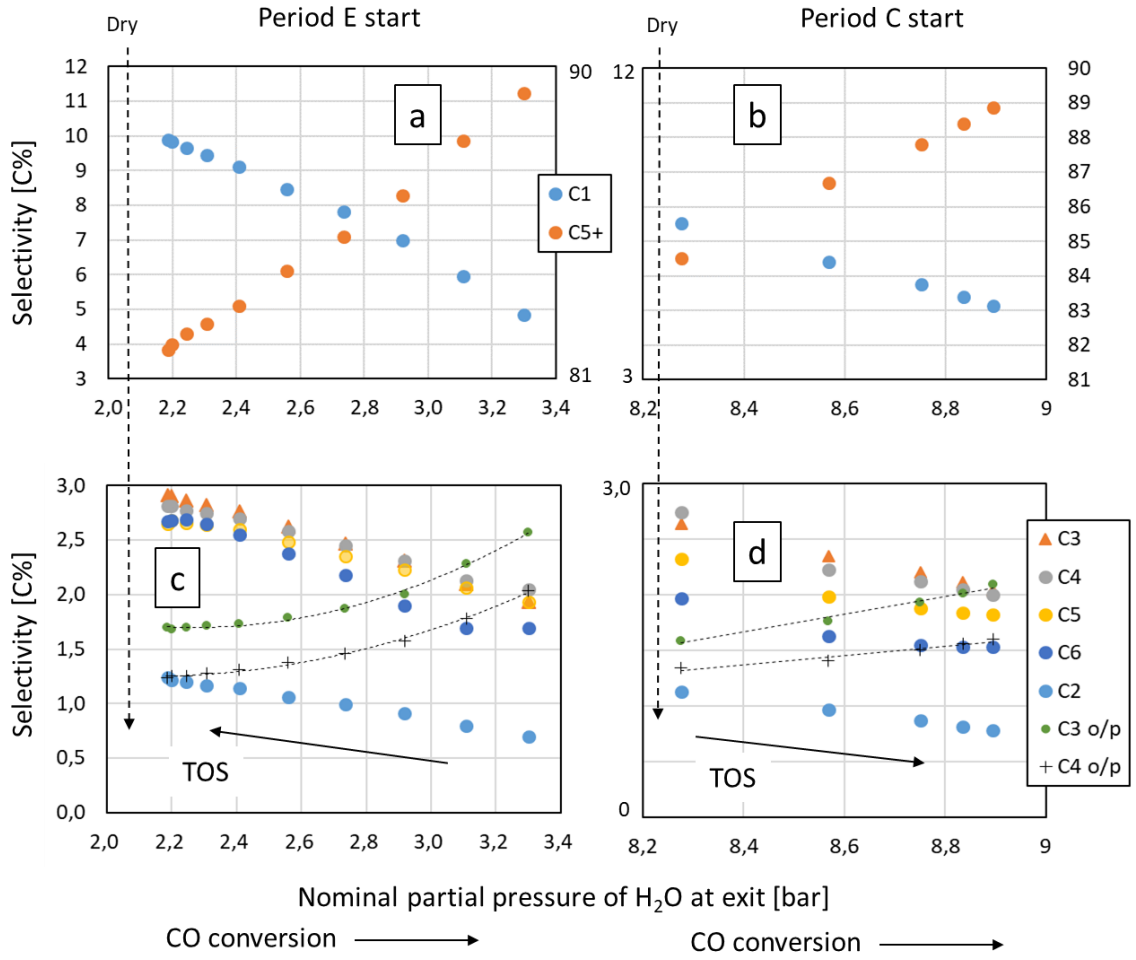

Figure 8. Carbon selectivities under transient water conditions during start of periods C and E for catalyst $C_{\alpha 1}$. a) and b): selectivities to methane and C_{5+}. c)and d): selectivities to C_2-C_6 chains.

Activity and selectivities in Figures 5 and 6 show that there are transient periods of ca. 5 and 10 hrs., respectively, after water is added in the beginning of period C and removed in the onset of period E. There are positive responses to water on activity and selectivity to higher hydrocarbons that are reversed as water is removed. Further analyses of these transient periods are given in Figure 8 where selectivities are plotted as a function of water vapor pressure calculated as the sum of water in feed and water generated indigenously through the reactor. This means that the shown response to water also represents CO conversion to a good approximation. The mechanism of the transients can be due to one of the following: gas mixing in feed lines or in the reactor bed; diffusion of water in the catalyst pores; equilibration of the cobalt crystallite surface; oxidation/reduction reactions. Extra-particle gas mixing and cobalt surface equilibration are found to be faster than the time scale under consideration; confer *e.g.* the A→B transition in Figures 5 and 6 and experience from SSITKA and AFM measurements. On the other hand, oxidation or reduction of cobalt are found to be reasonably slow processes as seen by deactivation through periods C and D, and catalyst activation. We therefore conclude that diffusion of water in the catalyst pores plays a major role, although we cannot exclude some overlap with other mechanisms. In particular, there is some uncertainty regarding the effect of residual water in the vaporizer. Water is fed separately from the syngas, and the water flow is stopped or started by a valve in front of the gasifier. An indication that this residual

water has minimal effect on the transients is the significant differences in transient duration between test periods B and E. A calculation based on the volume of the vaporizer and plug-flow exchange of gases indicates that water is added or removed from the reactor feed gas in less than ½ h. Therefore, as the water vapor pressure gradually penetrates the catalyst pellets, activity of the α-alumina supported cobalt catalyst increases. It is a synergistic effect whereby water diffusion gives higher CO conversion, which in turn produces more water. Note, however, that the 1.1 and 0.6 bar changes in nominal P_{H2O} due to conversion change through the transition periods are only ca. 1/7 of the amount of water added in periods D and C; 7.06 and 4.25 bar, respectively. Consequently, pore diffusion is most important. Due to the nearly double water concentration change in transition period E compared to C, the double length of the E period follows nicely as do the double response to conversion.

From the above derivation it also follows that the start of period C and the end of the transition part of period E represent dry syngas at the cobalt sites. The most striking observation is that all selectivity responses are linear to the nominal water partial pressure; *i.e.* to CO conversion. This might be expected from previous studies on FTS where water is found to be the key to activity and selectivity,[28] and also suggested to be active in CO activation.[19] Nevertheless, it is again pointed out that pore diffusion has a much higher impact than conversion itself.

The deactivated catalyst in the transient of period E shows some characteristic selectivity features compared to the fresh catalyst in period C:

- There is significantly more methane formed during the transient in period E, rising from 5 to 10 C%, although the values are approximately the same at the water rich conditions in the start of period E and end of period C.
- The reduction of S_{C5+} between the two dry periods is ΔC of 2.5%, equal to the methane increase; implying minimal change in C_2-C_4 products.
- Although the C_2-C_4 fraction is similar at the water rich conditions in both periods, there is more C_5 and C_6 when water is removed in period E compared to the start of period C.
- The olefin to paraffin ratio is, as expected, highest under wet conditions. This ratio decreases more rapidly during drying, from a higher level, of the deactivated catalyst compared to the trend when water is added to the fresh catalyst.
- The selectivity to CO_2 increases gradually from 1.17 to 1.47 C% when water is added, while it is almost constant during transient period E at 1.22±0.07 C%.

The data indicate that the deactivated catalyst gives rise to more methane and at the same time a lower chain growth probability. These observations are reasonable as the conversion is reduced with consequently less water formed; and it is known that water impacts all chain growth probabilities, with the largest increase being in α_1. Further, it was recently shown that α-alumina supported catalysts respond more strongly to water than γ-alumina supported ones,[28] see also below. The selectivities follow the expectations from measured olefin/paraffin ratios. As a predominantly secondary reaction, hydrogenation of olefins depends largely on residence time and hydrogen coverage. Dilution with water in the feed gives higher surface coverage of H_2O/OH- at the expense of H_2. Therefore, added water suppresses the hydrogenation reaction. All in all, the selectivity behavior of the deactivated catalyst is well rationalized. The nature of the deactivation does not seem to cause erratic selectivity behavior, indicating that any cobalt crystallite size effects due to oxidation or sintering are outside the present experimental range; *c.f.* Table 1. There is one possible exception; the stability observed for CO_2 selectivity of the deactivated catalyst.

Selectivity comparison with γ-alumina

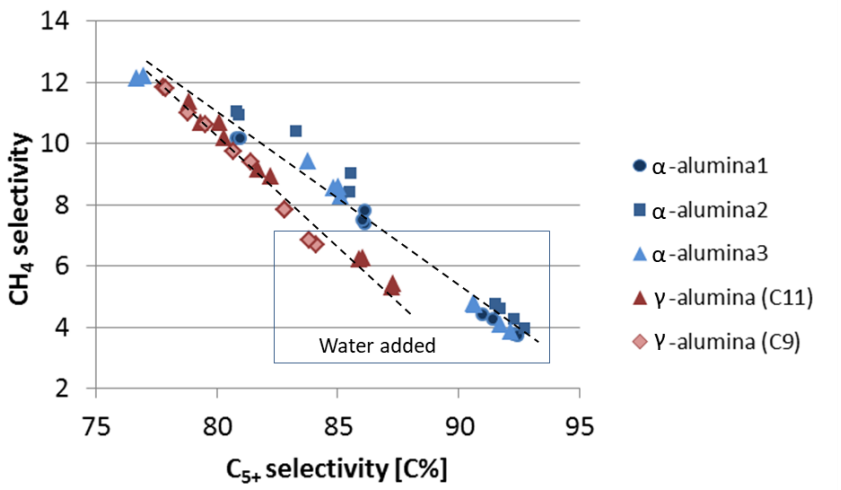

Figure 9. Methane selectivity plotted as function of C_{5+} selectivity for catalysts $C_{\alpha 1}$, $C_{\alpha 2}$, $C_{\alpha 3}$, C_{γ} (C11 and C9). Data points are for start and end of each test period.

A linear response between CH_4 and C_{5+}, as in Figure 9 where data for all five test periods have been collected, was previously taken as a verification of the CH_x pool model. Methane and higher hydrocarbons are interlinked and do not proceed through entirely independent reactions. Evidently, periods with water addition falls in the line sections with highest S_{C5+}. For the first time we have been able to separate these correlations based on type of support. High C_{5+} selectivity for catalysts on α-alumina, particularly for conditions with high water concentration, can partly be explained by a shift downward and to the right along lines in the diagram. (The position of the two upper data points for one α sample is due to particularly low conversion in startup period A for this test). The mechanistic rationale behind this shift is preferential CO activation with water for larger cobalt crystals assumed to have a more ordered structure that are less prone to strain originating in the support-metal interphase. Most striking, however, is the sideways offset of the trendline, *i.e.* toward higher S_{C5+}. Analyzing the selectivity data further in terms of Anderson-Shultz-Flory propagation probabilities (α) for the first insertions will give further insight into the mechanistic origin of the offset, particularly whether chain initiation (α_{C1}) or propagation (α_{C4}) are influenced the most.

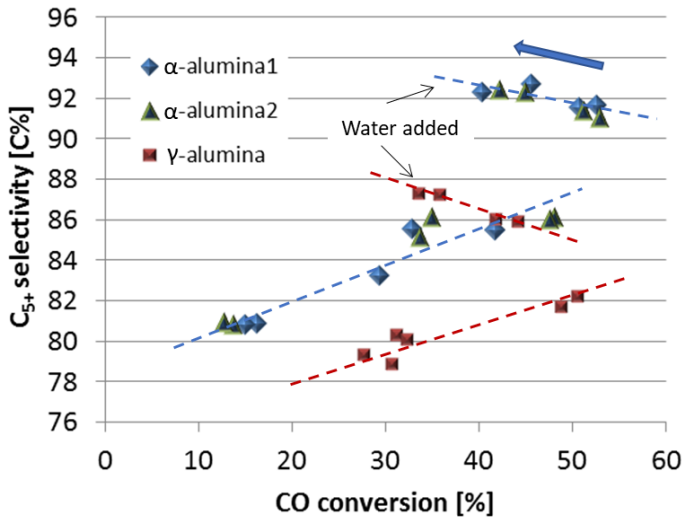

Figure 10. Plot of C_{5+} selectivity *vs.* CO conversion for catalysts $C_{\alpha 1}$, $C_{\alpha 2}$, and C_{γ}. There are 10 data points for each catalyst corresponding to start and end of each test period.

It has been implied above that there is a link between CO conversion (activity) and C_{5+} selectivity. That conditions favoring high selectivity when water is added also promotes activity was clearly demonstrated recently.[29] A straight line (R^2=0.93) was obtained by plotting the change in S_{C5+} *vs.* change in CO conversion when comparing test periods C with B for 14 catalysts on different alumina supports, including α-alumina. Further verification of the selectivity/activity dependence can be deduced from Figure 10. Straight lines are obtained for all catalysts categorized in terms of support type. The trends in the dry periods A, B and E follows simply from differences in CO conversion and the corresponding level of indigenously generated water. The trends are obviously reversed when water is added in periods B and C. This is explained as follows: When a large concentration of water is experienced in period E, the conversion drops, partly due to deactivation and partly due to low syngas pressure; still, the positive effect on selectivity is maintained.

Chain propagation probabilities

Probabilities for chain growth, specifically α_1, α_2, α_3 and α_4, have been calculated from measured selectivities by a procedure described previously.[57] These probabilities describe the following steps of chain initiation and propagation: α_1; fraction of CH_x monomers that combine with another monomer to give C_2H_y, *i.e.* initiating chain growth, relative to being hydrogenated to CH_4. α_2; fraction of C_2H_y that picks up a new monomer to give a C_3 moiety relative to being terminated. α_3 and α_4; probabilities of the first steps of chain propagation relative to termination. A critical factor dictating α_1 is hydrogen coverage on the cobalt surface, whereas hydrogen, according to our mechanistic model,[19] does not influence higher α values as hydrogen participates both in chain growth and termination. Note that C_2H_y is different in chemical nature from subsequent longer chains in that a very low portion terminates, and then to ethane.

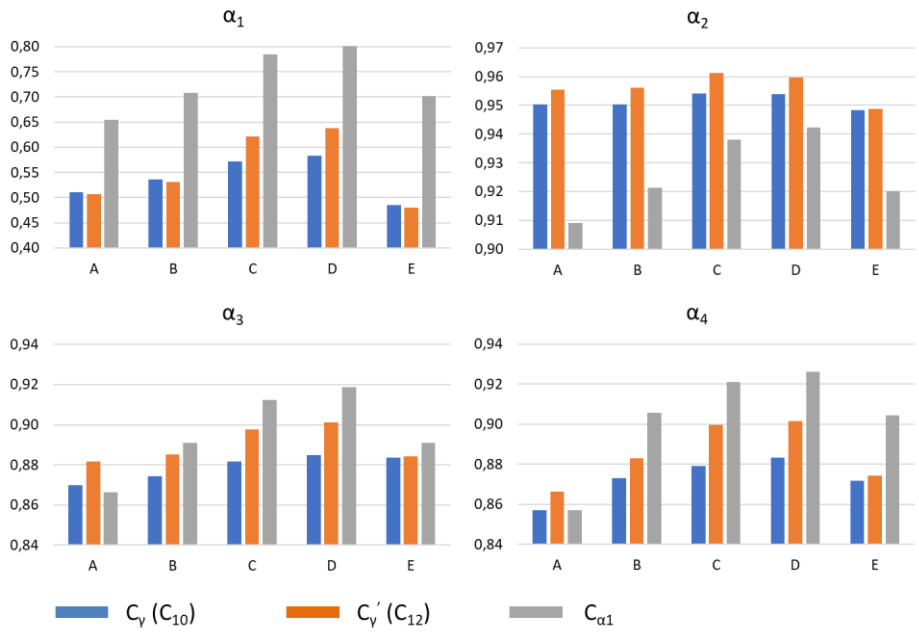

Figure 11. Chain propagation probabilities α_1, α_2, α_3 and α_4 in end of test periods A to E for two γ-alumina and one α-alumina supported catalysts. Catalyst notations in brackets refer to numbering in refs. 25 and 29; C_{10}: average pore diameter 11.6 nm, C_{12}: 18.3 nm.

Figure 11 contains a comparison of probabilities for two γ-alumina supported Co-catalysts and one α-alumina based. The γ-alumina supported catalysts have rather different pore diameters, 11.6 and 18.3 nm, characteristic of medium/large and very large pore materials, respectively. We documented recently that very large pores in γ-alumina favors positive water response for both activity and selectivity. Successive positive development of all four chain-growth probabilities for each of the three supports in the test sequence A→D is evident from the figure. This correlates without exception with increase in water vapor pressure. Except for α_2, there is also systematic increase in α-values in the catalyst sequence $C_\gamma \rightarrow C_\gamma' \rightarrow C_{\alpha 1}$ as the crystals of the support becomes larger, and presumably more inert. The apparent deviation in period A for the higher α-values is fortuitous due to only half the conversion for $C_{\alpha 1}$ at a given GHSV as the cobalt dispersion is low; see Table 1. Be aware of the different scales in the subfigures; the scale for α_1 being compacted significantly. In other words, both water and type of support influence α_1 the most. This is partly in line with previous results for a series of 13 different γ-alumina supported catalysts.[29] Exceptions are evident looking at the dry feed periods B and E where the γ-alumina supports respond to the pore structure by increase in α_3 and α_4, leaving α_1 unchanged. A further apparent inconsistency is that the catalyst on α-alumina show reduced probability compared to γ-alumina for the $C_2 \rightarrow C_3$ chain growth step, *i.e.* for α_2. A tentative interpretation is that when there is a large number of initiated growing chains, high α_1, some of these are in unfavorable surface configurations for further growth. A high water/hydroxyl concentration evidently is able to relieve the locked configuration to some extent. This double effect of water, *i.e.* both on α_1 and α_2, likely is the root cause behind the positive displacement of the trendline for α-support in Figure 9. Unique properties of catalysts on α-alumina then are:

- Very high α_1 values at all process conditions
- Low α_2 that respond positively to water vapor concentration
- Higher α_3 and α_4 probabilities that follow trend from γ-alumina supports.

There are presumably several types of modification of the cobalt crystallites that may occur in the sequence; medium/large pore γ-alumina, very large pore γ-alumina and to α-alumina. First, the crystallite size increases as a consequence of incipient wetness impregnation if no special measures are taken. Second, less strain is introduced on Co due to larger support crystallites. Third, a more inert support surface suppresses formation of pronounced cobalt-oxide metal-support interphases. Fourth, these changes may lead to more regular cobalt crystals with less stacking faults. There is also a possibility of transition from *fcc* to *hcp* stacking of the cobalt atoms. Without having access to more advanced characterization of the materials, also *in operando* when water is added, it is only concluded that more well-defined cobalt crystals tend to improve the selectivity to higher hydrocarbons. This also follows from of a recent FTS study showing that more regular cobalt crystallites outperform nano-particles with more pronounced lattice defects.[17] The reason for the derived correlation was found to be lower hydrogen surface coverage and presumably easier generation of monomers, in line with the discussion above. Therefore, we favor the hypothesis that more regular supports like α-alumina, and presumably titania, suppress hydrogen coverage due to less defects in the crystal structure of cobalt. Note, however, that a moderate volcano plot appears for C_{5+} selectivity *vs.* crystallite size, irrespective of support type.[58]

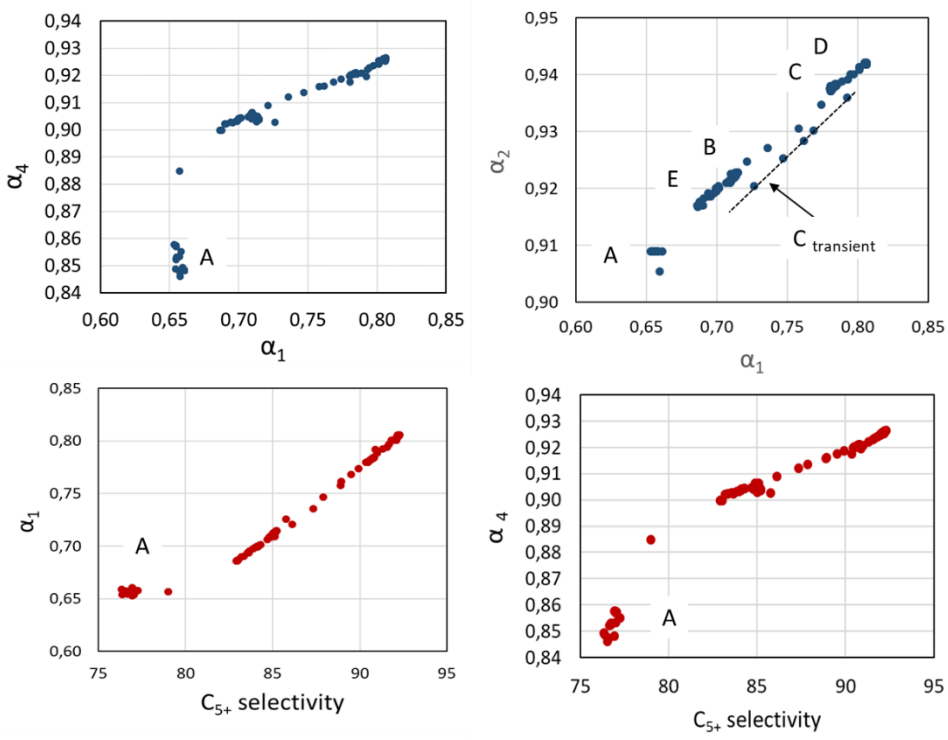

Figure 12. Correlations between chain growth probabilities and selectivity to C_{5+} for the catalyst $C_{\alpha 1}$.

Further details of chain growth probabilities, considering all experimental data-points, are given in Figure 12 for catalyst $C_{\alpha 1}$. The most striking observation is that any correlation between the parameters α_1, α_2, α_4 and S_{C5+} give linear trends; leaving out period A. This period is characterized by very low CO conversion in the 10% range due to high initial GHSV, *ref.* Figure 5, with subsequent particularly low water concentration in the syngas. This condition evidently results in higher α_1 than expected, but still lowest observed, and lower α_4 than anticipated from the trendline. The short residence time manifests itself in reduced re-adsorption of olefins with a resulting high olefin to paraffin ratio. There is also a slight, but systematic, deviation for the transient in period C when water is added characterized by low α_1 and α_2. This is ascribed to the gradual diffusion of water described above toward saturation of all cobalt surfaces. Still, the general linear correlations are further evidence for an FTS mechanism that interlinks all products, including methane.[19]

Conclusion

From the results based on Fischer-Tropsch synthesis of cobalt catalysts on α-alumina supports, including addition of water to the feed, we conclude the following:

1. Both activity and selectivity to higher hydrocarbons respond positively to water added or generated *in situ* by the reaction.
2. There is a linear trend between formation of methane and C_{5+} products, but displaced to higher C_{5+} values for α-alumina supports compared to catalysts on γ-alumina.
3. Calculation of chain propagation probabilities (α_n) for α-alumina supported catalysts discloses that the first step, characterized by α_1, increases the most under higher water partial pressure.

4. α_1 is significantly higher for α-compared to all γ-alumina supports irrespective of pore sizes of the latter.
5. The results are ascribed to suppression of hydrogen coverage on the cobalt surface, linked to more regular cobalt crystallites, accompanied by enhanced water assisted generation of CH_x polymerization monomers.
6. The α_2 probability is surprisingly low for α-alumina supports, although it increases significantly with water concentration.
7. Linear correlations are found between each pair of parameters α_1, α_2, α_4 and S_{C5+}; giving support to a mechanistic model where all products are interlinked, including methane.
8. Transients observed when water is added or removed from the system are ascribed to pore diffusion. Selectivities in these periods follow closely the general selectivity trends found for different process conditions

References

[1] Bezemer, G. L.; Bitter, J. H.; Kuipers, H. P. C. E.; Oosterbeek, H.; Holewijn, J. E.; Xu, X.; Kapteijn, F.; van Dillen, A. J.; de Jong, K. P. Cobalt Particle Size Effects in the Fischer-Tropsch Reaction Studied with Carbon Nanofiber Supported Catalysts. *J. Am. Chem. Soc.* **2006**, *128*, 3956.

[2] Borg, Ø; Dietzel, P. D. C.; Spjelkavik, A. I.; Tveten, E. Z.; Walmsley, J. C.; Eri, S.; Holmen, A.; Rytter, E. Fischer-Tropsch Synthesis: Cobalt Particle Size and Support Effects on Intrinsic Activity and Product Distribution *J. Catal.* **2008**, *259*, 161.

[3] B. C. Enger, Å.-L. Fossan, Ø. Borg, E. Rytter, A. Holmen, J. Catal. 284 (2011) 9.

[4] Borg, Ø.; Walmsley, J. C.; Dehghan, R.; Tanem, B. S.; Blekkan, E. A.; Eri, S.; Rytter, E.; Holmen, H. Electron Microscopy Study of γ–Al_2O_3 Supported Cobalt Fischer-Tropsch Catalysts *Catal. Lett.* **2008**, *126*, 224.

[5] Arsland, I.; Walmsley, J.; Rytter, E.; Bergene, E.; Midgley, P. Toward Three-Dimensional Nano-Engineering of Heterogeneous Catalysts, *J. Am. Chem. Soc.* **2008**, *130*, 5716-5719.

[6] Ducreax, O.; Rebours, B.; Lynch, J.; Roy-Auberger, M.; Bazin, D. Microstructure of Supported Cobalt Fischer-Tropsch Catalysts. Oil & Gas Sci. Tech.-Rev. IFP **2009**, *64*, 49.

[7] N. E. Tsakoumis, E. Patanou, S. Lögdberg, R. E. Johnsen, R. Myrstad, W. van Beek, E. Rytter and E. Blekkan, submitted.

[8] Mauldin, C. H. Cobalt Catalysts for the Conversion of Methanol to Hydrocarbons and for Fischer-Tropsch Synthesis. Patent: *United States Patent 4,568,663*, 1986.

[9] Eri, S.; Goodwin, J.; Marcelin, G.; Riis, T. Catalyst for production of hydrocarbons. *United States Patent 4.801.573*, 1987.

[10] Mauldin, C. H.; Varnado, D. E. Rhenium as a Promoter of Titania-Supported Cobalt Fischer-Tropsch Catalysts. *Stud. Surf. Sci. Catal.* **2001**, *136*, 417.

[11] Hilmen, A-M.; Schanke, D.: Holmen, A. TPR Study of the Mechanism of Rhenium Promotion of Alumina-Supported Cobalt Fischer-Tropsch Catalysts. *Catal. Lett.* **1996**, *38*, 143.

[12] F. Diehl and A.Y. Khodakov, Promotion of Cobalt Fischer-Tropsch Catalysts with Noble Metals: a Review, Oil & Gas Sci. Tech.-Rev. IFP **2009**, *64*, 11-24.

[13] Storsæter, S.; Borg, Ø.; Blekkan, E. A.; Tøtdal, B.; Holmen, A. Fischer-Tropsch Synthesis over Re-Promoted Co Supported on Al_2O_3, SiO_2 and TiO_2: Effect of Water. *Catal. Today* **2005**, *100*, 343.

[14] Jacobs, G.; Das, T. K.; Patterson, P. M.; Li, J.; Sanches, L.; Davis, B. H. Fischer-Tropsch Synthesis: XAFS Studies of the Effect of Water on a Pt-Promoted Co/Al_2O_3 Catalyst. *Appl. Catal A.* **2003**, *247*, 335.

[15] Schanke, D.; Hilmen, A. M.; Bergene, E.; Kinnari, K.; Rytter, E.; Ådnanes, E.; Holmen, A. Study of the Deactivation Mechanism of Al_2O_3-Supported Cobalt Fischer-Tropsch Catalyst. *Catal. Lett.* **1995**, *34*, 269.

[16] Blekkan, E. A.; Borg, Ø.; Frøseth, V.; Holmen, A. Fischer-Tropsch Synthesis on Cobalt Catalysts: The Effect of Water. In: Catalysis. Cambridge, UK: The Royal Society **2007**,13.

[17] N. E. Tsakoumis, J. C. Walmsley, M. Rønning, W. van Beek, E. Rytter, A. Holmen, *J. Am. Chem. Soc.* **2017**, *139*, 3706–3715.

[18] W. Ma, G. Jacobs, Y. Ji, T. Bhatelia, D.B. Bukur, S. Khalid, B.H. Davis, Fischer–Tropsch synthesis: influence of CO conversion on selectivities, H_2/CO usage ratios, and catalyst Stability for a Ru promoted Co/Al_2O_3 catalyst using a slurry phase reactor, Top. Catal. 54 (2011) 757.

[19] E. Rytter and A. Holmen, Consorted vinylene mechanism for cobalt Fischer-Tropsch synthesis encompassing water or hydroxyl assisted CO-activation, Topics Catal., 61 (2018) 1024-1034.

[20] E. Rytter and A. Holmen, Perspectives on the Effect of Water in Cobalt Fischer–Tropsch Synthesis**,** ACS Catal. 7(8) (2017) 5321-5328.

[21] Ø. Borg, S. Storsæter, S. Eri, H. Wigum, E. Rytter and A. Holmen, Catal. Lett. 107 (2006) 95

[22] Hibbits DD, Loveless BT, Neurock M, Iglesia E (2013) Angew
Chem Int Ed 20:12273–12278

[23] Brett T. Loveless, Corneliu Buda, Matthew Neurock and Enrique Iglesia: CO Chemisorption and Dissociation at High Coverages during CO hydrogenation on Ru Catalysts. JACS 135 (2013) 6107-6121

[24] Rytter, E.; Eri, S.; Schanke, D. Fischer-Tropsch Catalysts. Patent Application: International Publication *Number WO04/043596 A2,* 2004.

[25] Borg, Ø.; Eri, S.; Storsæter, S.; Blekkan, E. A.; Wigum, H.; Rytter, E.; Holmen, A. Fischer–Tropsch Synthesis over γ-Alumina-Supported Cobalt Catalysts: Effect of Support Variables. *J. Catal.* **2007**, *248*, 89.

[26] Eri, S.; Rytter, E. Cobalt and Rhenium Containing Fischer-Tropsch Catalysts. Patent Application: *International Publication Number WO06/010936 A1*, 2006.

[27] Rane, S.; Borg, Ø.; Rytter, E.; Holmen, A. Relation Between Hydrocarbon Selectivity and Cobalt Particle Size for Alumina Supported Cobalt Fischer-Tropsch Catalysts. *Appl. Catal. A* **2012**, *437-438*,10-17.

[28] S. Krishnanmoorthy, M. Tu, M.P. Ojeda, D. Pinna and E. Iglesia: An investigation on the effects of water on the rate and selectivity for the Fischer-Tropsch synthesis on cobalt-based catalysts. J. Catal 211(2) (2002) 422-433

[29] E. Rytter, N. Tsakoumis and A. Holmen, Water as key to activity and selectivity in Co Fischer-Tropsch synthesis: γ-alumina based structure-performance relationships, J. Catal. 365 (2018) 334-343.

[30] Saib, A. M.; Claeys, M.; van Steen, E. Silica Supported Cobalt Fischer-Tropsch Catalysts: Effect of Pore Diameter of Support. *Catal. Today* **2002**, *71*, 395.

[31] L. Fratalocchi, C.G Visconti; L. Lietti, G. Groppi, E. Tronconi, E. Roccaro and R. Zennaroi: On the performance of a Co-based catalyst supported on modified γ-Al_2O_3 during Fisvher-Tropsch synthesis in the presence of co-fed water. Catal. Sci. Technol. 6 (2016) 6431-6440

[32] Lee, W. H.; Bartholomew, C. H. Multiple Reaction States in CO Hydrogenation on Alumina-Supported Cobalt Catalysts. J. Catal. **1989**, 120, 256.

[33] N. E. Tsakoumis, R. E. Johnsen, W. van Beek, M. Rønning, E. Rytter and A. Holmen,

Capturing metal-support interactions in situ during the reduction of a Re promoted Co/γ-Al_2O_3 catalyst, Roy. Soc. Chem., Chem. Com., 52 (2016) 3239-3242.

[34] Eri, S.; Kinnari, K. J.; Schanke, D.; Hilmen, A.-M. Fischer-Tropsch Catalyst with Low Surface Area Alumina, its Preparation and Use Thereof. Patent application: *International Publication Number WO 02/47816 A1*, 2002.

[35] Schanke, D.; Eri, S.; Rytter, E.; Aaserud, C.; Hilmen, A.-M.; Lindvåg, O. A.; Bergene, E.; Holmen, A. Fischer-Tropsch Synthesis on Cobalt Catalysts Supported on Different Aluminas. *Stud. Surf. Sci. Catal.* **2004**, *147*, 301.

[36] Ilke Arsland, John Walmsley, Erling Rytter, Edvard Bergene, Paul Midgley, *Toward Three-Dimensional Nano-Engineering of Heterogeneous Catalysts*, J. Am. Chem. Soc. 130(17) (2008) 5716-5719.

[37] Roya Dehghan-Niri, Thomas W. Hansen, Jacob B. Wagmer, Erling Rytter, Anders Holmen, John Walmsley: *In-situ reduction of cobalt oxide supported on alumina by environmental transmission electron microscopy*, Catal. Lett., 141 (2011) 754-761.

[38] E. Rytter and A. Holmen, Catal. Today, 275 (2016) 11-19.

[39] E. Rytter, A. Holmen, Catalysts 5 (2015) 478.

[40] E. Ochoa-Fernández, D. Chen, Z. Yu, B. Tøtdal, M. Rønning, A. Holmen, Surf. Sci. 554 (2004) L107

[41] S.P. Rane, Ø. Borg, J. Yang, E. Rytter, A. Holmen, Appl. Catal. A 388 (2010) 160.

[42] Borg, Ø.; Hammer, N.; Eri, S.; Lindvåg, O. A.; Myrstad, R.; Blekkan, E. A.; Rønning, M.; Rytter, E.; Holmen, A. Fischer-Tropsch Synthesis over Un-Promoted and Re-Promoted γ–Al_2O_3 Supported Cobalt Catalysts with Different Pore Sizes. *Catal. Today* **2009**, *142*, 70.

[43] Borg, Ø.; Blekkan, E. A.; Eri, S.; Akporiaye, D.; Vigerust, B.; Rytter, E.; Holmen, A. Effect of Calcination Atmosphere and Temperature for γ-Al_2O_3 Supported Cobalt Fischer-Tropsch Catalysts. *Top. Catal.* 45 (2007) 39-43.

[44] E.P. Barrett, L.G. Joyner and P.P. Halenda, J. Am. Chem. Soc. 73 (1951) 373.

[45] A.Y. Khodakov, J. Lynch, D. Bazin, B. Rebours, N. Zanier, B. Moisson and P. Chaumette, J. Catal. 168 (1997) 16.

[46] S. Storsæter, Ø. Borg, E.A. Blekkan and A. Holmen, Study of the effect of water on Fischer-Tropsch synthesis over supported cobalt catalysts, J. Catal. 231 (2005) 405-419.

[47] Ø. Borg, Z. Yu, D. Chen, E.A. Blekkan, E. Rytter and A. Holmen, The effect of water on the activity and selectivity for carbon nanofiber supported cobalt Fischer-Tropsch Catalysts, Top. Catal. 57 (2014) 491-499.

[48] C.E. Kliever, G. Kiss and G.J. DeMartin, Microscopy and Microanalysis 12 (2006) 135.

[49] D.J. Moodley, J. van de Loosdrecht, A.M. Saib, M.J. Overett, A.K. Datye, and J.W. Niemantsverdriet, Appl. Catal. 354 (2009) 102.

[50] M. Claeys, M. E. Dry, E. van Steen, P. J. van Berge, S. Booyens, R. Crous, P. van Helden, J. Labuschagne, D. J. Moodley, A. M. Saib, *ACS Catal.* **2015**, *5*, 841–852.

[51] N. E. Tsakoumis, R. Dehghan-Niri, M. Rønning, J. C. Walmsley, Ø. Borg, E. Rytter, A. Holmen, *Appl. Catal. A Gen.* **2014**, *479*, 59–69.

[52] J. Li, X. Zhan, Y. Zhang, G. Jacobs, T. Das and B. H. Davis, Appl. Catal. A 228 (2002) 203.

[53] C.E. Kliewer, S.L. Soled and G. Kiss, Catal. Today, 2018, in press. https://doi.org/10.1016/j.cattod.2018.05.021.

[54] Moodley, D.J.; van de Loosdrecht, J.; Saib, A.M.; Overett, M.J.; Datye, A.K.; Niemantsverdriet, J.W. Carbon deposition as a deactivation mechanism of cobalt-based Fischer–Tropsch synthesis catalysts under realistic conditions. *Appl. Catal.***2009**, *354*, 102–110.

[55] S. Lögdberg, J. Yang, M. Lualdi, J.C. Walmsley, S. Järås, M. Boutonnet, E.A. Blekkan, E. Rytter and A. Holmen, J. Catal. 352C (2017) 515-531.

[56] C.J. Bertole, C.A. Mims and G. Kiss, J. Catal. 221 (2004) 191.

[57] S. Lögdberg, M. Lualdi, S. Järås, J.C. Walmsley, E.A. Blekkan, E. Rytter, A. Holmen, *On the selectivity of cobalt-based Fischer-Tropsch catalysts: evidence for a common precursor for methane and long chain hydrocarbons*, J. Catal. 274 (2010) 84.

[58] Erling Rytter, Nikolaos E. Tsakoumis and A. Holmen, *On the Selectivity to Higher Hydrocarbons in Co-based Fischer-Tropsch Synthesis*, Cat. Today 261 (2016) 3-16.